

This is the accepted manuscript made available via CHORUS. The article has been published as:

Heavy-quark-state production in p-p collisions

Leonard S. Kisslinger, Ming X. Liu, and Patrick McGaughey

Phys. Rev. D **84**, 114020 — Published 16 December 2011

DOI: [10.1103/PhysRevD.84.114020](https://doi.org/10.1103/PhysRevD.84.114020)

Heavy Quark State Production In p-p Collisions

Leonard S. Kisslinger

Department of Physics, Carnegie Mellon University, Pittsburgh, PA 15213

Ming X. Liu and Patrick McGaughey

P-25, Physics Division, Los Alamos National Laboratory, Los Alamos, NM 87545

Abstract

We estimate the relative probabilities of $\Psi'(2S)$ to J/Ψ production at BNL-RHIC and $\Upsilon(nS)$ production at the LHC and Fermilab in p-p collisions, using our recent theory of mixed heavy quark hybrids, in which the $\Psi'(2S)$ and $\Upsilon(3S)$ mesons have approximately equal normal $q\bar{q}$ and hybrid $q\bar{q}g$ components.

PACS Indices:12.38.Aw,13.60.Le,14.40.Lb,14.40.Nd

1 Introduction

There has been a great deal of interest in the production and polarization of heavy quark states in proton-proton collisions. This was motivated in part by the $J/\Psi, \Psi'$ production anomaly[1], in which the charmonium production rate was larger than predicted for J/Ψ , and much larger for Ψ' than theoretical predictions in proton-proton (p-p) collisions; and the disagreement between experimental measurements of polarization of $J/\Psi, \Psi'$ [2] states produced at high energy and theoretical predictions[3]. In addition to being an important study of QCD, it also could provide the basis for testing the production of Quark Gluon Plasma (QGP) in relativistic heavy ion collisions (RHIC). We use the notation $E=\sqrt{s}$.

At the proton-proton (p-p) energies of the Fermilab, BNL-RHIC, or the Large Hadron Collider the color octet model[3, 4, 5] dominates the color singlet model, as was shown in studies of J/Ψ production at $E=200$ GeV at BNL[6, 7]. In this color octet model heavy quark state production cross sections require partonic distributions and nonperturbative matrix elements. In our present work we use this framework, but some of our nonperturbative matrix elements are taken from a recent publication[8] in which it was shown that some of the charmonium and upsilon states are mixed meson and hybrid meson states, which followed the work in which it was shown that these states are not pure hybrids[9]. This is particularly important for the application of the octet model, since the heavy quark $Q\bar{Q}$ in a hybrid are in a color octet representation. The mixed hybrid model of Ref[8] can also explain the $\Psi'(2S)$ production anomaly, with a much larger production of $\Psi'(2S)$ in high energy collisions than standard model predictions[10], the famous $\rho - \pi$ puzzle, and the anomalous production of sigmas in the decay of $\Upsilon(3S)$ to $\Upsilon(1S)$ [11]. In section 2 we discuss mixed heavy quark hybrids and the solution to these puzzles.

In the present work on heavy quark state production in p-p collisions we estimate the relative production of $\Psi'(2S)$ to J/Ψ at BNL-RHIC (200 GeV)[6, 7], and the relative production of $(\Upsilon(2S) + \Upsilon(3S))$, $\Upsilon(1S)$ states at the Large Hadron Collider (2.76 TeV)[12], and $(\Upsilon(nS))$ states at Fermilab (38.8 GeV)[13, 14].

We closely follow the formulation of Nayak and Smith[15] in which they calculated J/Ψ and $\Psi'(2S)$ production, produced by unpolarized or polarized p-p collisions at $\sqrt{s} = 200$ GeV for helicity $\lambda = 0$ and $\lambda = 1$. We generalize this by considering the production of a heavy quark state Φ , where Φ is Charmonium $J/\Psi, \Psi'$ or Bottomonium $\Upsilon(nS)$. It is important to note that in Ref[8] the $\Psi'(2S)$ and $\Upsilon(3S)$ were found to be approximately 50% a heavy quark meson and 50% a hybrid.

2 Review of mixed hybrid heavy quark mesons

The Charmonium and Upsilon (nS) states which we are studying are shown in Figure 1

Figure 1: Lowest energy Charmonium and Upsilon states

2.1 Heavy quark meson decay puzzles

Note that the standard model of the $\psi'(2S)$ and $\Upsilon(3S)$ as $c\bar{c}$ and $b\bar{b}$ mesons is not consistent with the following puzzles:

1) The ratio of branching ratios for $c\bar{c}$ decays into hadrons (h) given by the ratios (the wave functions at the origin canceling)

$$R = \frac{B(\Psi'(c\bar{c}) \rightarrow h)}{B(J/\Psi(c\bar{c}) \rightarrow h)} = \frac{B(\Psi'(c\bar{c}) \rightarrow e^+e^-)}{B(J/\Psi(c\bar{c}) \rightarrow e^+e^-)} \simeq 0.12 ,$$

the famous 12% RULE.

The $\rho - \pi$ puzzle: The $\Psi'(2S)$ to J/Ψ ratios for $\rho - \pi$ and other h decays are more than an order of magnitude too small. Many theorists have tried and failed to explain this puzzle.

2) The Sigma Decays of Upsilon States puzzle: The σ is a broad 600 MeV $\pi - \pi$ resonance.

$\Upsilon(2S) \rightarrow \Upsilon(1S) + 2\pi$ large branching ratio. No σ

$\Upsilon(3S) \rightarrow \Upsilon(1S) + 2\pi$ large branching ratio to σ

We call this the Vogel $\Delta n = 2$ Rule[11]. Neither of these puzzles can be solved using standard QCD models. We have solved them using the mixed heavy hybrid

2.2 Hybrid, mixed heavy quark hybrid mesons, and the puzzles

First, we used the method of QCD Sum Rules, starting with the vector hybrid current ($J^{PC} = 1^{--}$) for heavy quark hybrid mesons

$$J_{HH\mu} = \bar{q}_A^a \gamma^\nu \gamma_5 \frac{\lambda_{ab}^n}{2} \tilde{G}_{\mu\nu}^n q_B^b ,$$

where A,B are flavor indices, a,b are color indices, and $\tilde{G}_{\mu\nu}^n$ is the gluon field operator. The QCD Sum Rule method starts with the two-point correlator for a heavy hybrid

$$\Pi_{HH}^{\mu\nu}(q^2) = i \int d^4x e^{iq \cdot x} \langle 0 | T [J_{HH}^\mu(x) J_{HH}^\nu(0)] | 0 \rangle . \quad (1)$$

Using the $J_{HH\mu}$ hybrid current and the QCD Sum Rule method it was shown[9] that no low-lying charmonium state is a hybrid.

Then the mixed vector ($J^{PC} = 1^{--}$) charmonium, hybrid charmonium current

$$\begin{aligned} J^\mu &= b J_H^\mu + \sqrt{1-b^2} J_{HH}^\mu \text{ with} \\ J_H^\mu &= \bar{q}_c^a \gamma^\nu \gamma_5 q_c^a , \end{aligned}$$

where J_H^μ is the current for a 1^{--} charmonium state, and J_{HH}^μ is the heavy charmonium hybrid current given above, was tried[8]. A solution satisfying all QCD Sum Rule conditions was found for the $\Psi'(2S)$ to be a mixed heavy hybrid, with $b \simeq -.7$

$$|\Psi'(2S) \rangle = -0.7 |c\bar{c}(2S) \rangle + \sqrt{1-0.5} |c\bar{c}g(2S) \rangle . \quad (2)$$

Using this method for bottom quark mesons, it was found that the $\Upsilon(3S)$ state was a mixed hybrid:

$$|\Upsilon(3S) \rangle = -0.7 |b\bar{b}(3S) \rangle + \sqrt{1-0.5} |b\bar{b}g(3S) \rangle . \quad (3)$$

Therefore for both the $\Psi'(2S)$ and $\Upsilon(3S)$ $b=-.7$, and both have a 50% probability of being a hybrid and 50% probability of being a standard $q\bar{q}$ meson. In Ref[8] it was shown that this solves the $\Psi'(2S)$ to J/Ψ the $\rho - \pi$ puzzle, and the Vogel $\Delta n = 2$ Rule.

We now investigate how this mixed heavy hybrid meson theory affects the production of charmonium and upilon states via p-p collisions.

3 Unpolarized p-p collisions

The cross sections for J/Ψ and $\Psi'(2S)$ production in the color octet model are based on the cross sections obtained from the matrix elements for quark-antiquark and gluon-gluon octet fusion to a hadron H , $\sigma_{q\bar{q} \rightarrow H(\lambda)}$ and $\sigma_{gg \rightarrow H(\lambda)}$, with λ the helicity, as illustrated in Figure 2.

Figure 2: Gluon and quark-antiquark color octet fusion producing hadron H

In Ref[15] the matrix elements used were derived by Braaten and Chen[4]. The three octet matrix elements needed are $\langle O_8^\Phi(^1S_0) \rangle$, $\langle O_8^\Phi(^3S_1) \rangle$, and $\langle O_8^\Phi(^3P_0) \rangle$, with Φ either J/Ψ , $\Psi'(2S)$, or $\Upsilon(nS)$. Since these matrix elements are not well known, Nyyak and Smith[15] use three scenerios: 1) $\langle O_8^\Phi(^1S_0) \rangle = \langle O_8^\Phi(^3P_0) \rangle / m^2 = .0087$, 2) $\langle O_8^\Phi(^1S_0) \rangle = .039$ and $\langle O_8^\Phi(^3P_0) \rangle = 0$, 3) $\langle O_8^\Phi(^1S_0) \rangle = 0$ and $\langle O_8^\Phi(^3P_0) \rangle / m^2 = .01125$, with $\langle O_8^\Phi(^3S_1) \rangle = .0112$ in all scenerios and all having units GeV^3 . Note that these matrix elements are not used to obtain the wave functions of the heavy quark meson states.

To obtain the production cross sections one needs to multiply by the quark-antiquark or gluon parton distribution functions, giving

$$\begin{aligned} \sigma_{pp \rightarrow \Phi(\lambda)} &= \int_a^1 \frac{dx}{x} f_q(x, 2m) f_{\bar{q}}(a/x, 2m) \sigma_{q\bar{q} \rightarrow H(\lambda)} \\ &\quad + f_g(x, 2m) f_g(a/x, 2m) \sigma_{gg \rightarrow H(\lambda)} , \end{aligned} \quad (4)$$

where $a = 4m^2/s$, with $m = 1.5 \text{ GeV}$ for charmonium, and 5 GeV for bottomonium. $f_g(x, 2m)$, $f_q(x, 2m)$ are the gluonic and quark distribution functions evaluated at $Q = 2m$. First we consider unpolarized p-p collisions, using[15] scenerio 2. With scenerio 2 matrix elements the production cross sections[4, 15] for Φ for helicity $\lambda = 0$ and 1 are

$$\begin{aligned} \sigma_{pp \rightarrow \Phi(\lambda=0)} &= A_\Phi \int_a^1 \frac{dx}{x} f_g(x, 2m) f_g(a/x, 2m) \\ \sigma_{pp \rightarrow \Phi(\lambda=1)} &= A_\Phi \int_a^1 \frac{dx}{x} [f_g(x, 2m) f_g(a/x, 2m) + 0.613((f_d(x, 2m) f_{\bar{d}}(a/x, 2m) \\ &\quad + f_u(x, 2m) f_{\bar{u}}(a/x, 2m))] , \end{aligned} \quad (5)$$

with $A_\Phi = \frac{5\pi^3\alpha_s^2}{288m^3s} < O_8^\Phi(1S_0) >$, $a = 4m^2/s$; where $m = 1.5$ GeV for charmonium, and 5 GeV for bottomonium. $f_g(x, 2m)$, $f_q(x, 2m)$ are the gluonic and quark distribution functions evaluated at $Q = 2m$.

The main purpose of the present work is to explore the effects of matrix elements for $\Psi'(2S)$ and $\Upsilon(nS)$ with $n=2,3$. We compare our results with the hybrid model to the standard model. In the standard model the states are (nS) quark-antiquark states, and the ratios of the matrix elements for n greater than 1 is given by the squares of the wave functions. Note that the basis for the octet model being used is the nonrelativistic QCD model[3, 4, 5], with a model potential for the quark anti-quark interaction giving bound states. A harmonic oscillator potential can be used to approximately give the energies of the first few states, which is what is needed in the present work. For the octet matrix elements illustrated in Figure 1, however, one must use QCD directly, and we use the results of Refs.[3, 4, 5, 15] for these matrix elements.

To approximate the ratios of matrix elements in a nonrelativistic quark model for these heavy quark meson states we use harmonic oscillator wave functions[16], with $\Phi(1S) = 2\text{Exp}[-r/a_o]/a_o^{3/2}$, $\Phi(2S) = \Phi(1S)(1 - r/a_o)/2^{3/2}$, and $\Phi(3S) = \Phi(1S)(1 - 2r/3a_o + 2r^2/27a_o^2)/3^{3/2}$. Defining $N1 = \int |\Phi(2S)|^2$ divided by $\int |\Phi(1S)|^2$ for the 2S to 1S probability, and similarly $N2$ for the 3S to 1S probability, we find $N1=0.039$, $N2=0.0064$, $N3=N2/N1=.16$. This is a very rough estimate. The cross sections for the mixed hybrid states are enhanced, as explained below.

Therefore, we use $A_{\Psi'(2S)} = 0.039A_{J/\Psi(1S)}$, $A_{\Upsilon(2S)} = 0.039A_{\Upsilon(1S)}$, and $A_{\Upsilon(3S)} = 0.0064A_{\Upsilon(1S)}$ in the standard model. On the other hand in the mixed hybrid study both $\Psi'(2S)$ and $\Upsilon(3S)$ were found to be approximately 50% hybrids. In Ref[8] it was shown, using the external field method, that the octet to singlet matrix element was enhanced by a factor of π^2 compared to the standard model, as illustrated in Figure 3. For mixed hybrids we use an enhancement factor of 3.0

Figure 3: External field method for $\Psi'(2S)$ and $\Upsilon(3S)$ states

For differential cross sections we use the rapidity variable, y ,

$$\begin{aligned} y(x) &= \frac{1}{2} \ln \left(\frac{E + p_z}{E - p_z} \right); \text{ with } E = \sqrt{M^2 + p_z^2} \\ p_z &= \frac{\sqrt{s}}{2} \left(x - \frac{a}{x} \right), \end{aligned} \quad (6)$$

or

$$x(y) = 0.5 \left[\frac{m}{s} (\exp y - \exp(-y)) + \sqrt{\left(\frac{m}{s} (\exp y - \exp(-y)) \right)^2 + 4a} \right] \quad (7)$$

For the unpolarized proton collisions we use a polynomial fit to the parton distributions of Ref.[17]. Because of the wide range of values, in order to obtain a good polynomial fit to the parton distributions we limit the range of rapidity to $-1. < y < 1$.

For $Q=3$ GeV, with $m=\text{Charmonium mass} = 1.5$ GeV, from Eq(7), x has a range about 0.028 to 0.032, and a/x 0.008 to 0.015. We have derived the following expressions for the gluon (g), u and d quark, and antiquark distribution functions using QTEQ6 for $Q=3$ GeV, fitting the range $x=0.008$ to .004, which is needed for $\sqrt{s}=200$ GeV

$$\begin{aligned} f_g(x) &\simeq 1334.21 - 67056.5x + 887962.0x^2 \\ f_d(x) &\simeq 72.956 - 3281.1x + 42247.6x^2 \\ f_u(x) &\simeq 82.33 - 3582.36x + 45867.3x^2 \\ f_{\bar{u}}(x) &\simeq 55.98 - 2722.04x + 35641.2x^2 \\ f_{\bar{d}}(x) &\simeq 57.44 - 2757.05x + 36030.5x^2. \end{aligned} \quad (8)$$

For $Q=10$ GeV, $m=\text{Bottomonium mass}=5$ GeV, from Eq(7), x has a range about 0.05 to 0.08, and a/x 0.03 to 0.05. We have derived the following expressions for the gluon (g), u and d quark, and antiquark distribution functions using QTEQ6 for $Q=10$ GeV, fitting the range $x=0.03$ to .08, which is needed for $\sqrt{s}=38.8$ GeV and 2.76 TeV.

$$\begin{aligned} f_g(x) &\simeq 275.14 - 6167.6x + 36871.3x^2 \\ f_d(x) &\simeq 26.96 - 527.14x + 3119.13x^2 \\ f_u(x) &\simeq 32.92 - 604.38x + 3530.1x^2 \\ f_{\bar{u}}(x) &\simeq 16.64 - 377.53x + 2336.86x^2 \\ f_{\bar{d}}(x) &\simeq 17.81 - 390.64x + 2392.46x^2. \end{aligned} \quad (9)$$

The differential rapidity distribution for $\lambda = 0$ is given by

$$\frac{d\sigma_{pp \rightarrow \Phi(\lambda=0)}}{dy} = A_\Phi \frac{1}{x(y)} f_g(x(y), 2m) f_g(a/x(y), 2m) \frac{dx}{dy}, \quad (10)$$

while for $\lambda=1$

$$\begin{aligned} \frac{d\sigma_{pp \rightarrow \Phi(\lambda=1)}}{dy} &= A_\Phi \frac{1}{x(y)} [f_g(x(y), 2m) f_g(a/x(y), 2m) + 0.613(f_d(x(y), 2m) f_{\bar{d}}(a/x(y), 2m) \\ &\quad + f_u(x(y), 2m) f_{\bar{u}}(a/x(y), 2m))] \frac{dx}{dy}. \end{aligned} \quad (11)$$

3.1 Charmonium Production Via Unpolarized p-p Collisions at $E=\sqrt{s}= 200$ Gev at BNL-RHIC

First we consider unpolarized p-p collisions for $\sqrt{s} = 200\text{GeV}$ corresponding to BNL energy. We use scenerio 2[15], with the nonperturbative matrix elements given above. Therefore, $A_\Phi = \frac{5\pi^3\alpha_s^2}{288m^3s} < O_8^\Phi(^1S_0) > = 7.9 \times 10^{-4}\text{nb}$ for $\Phi=J/\Psi$ and $2.13 \times 10^{-5}\text{nb}$ for $\Upsilon(1S)$ heavy quark states; $a = 4m^2/s = 2.25 \times 10^{-4}$ for Charmonium and 2.5×10^{-3} for Bottomium.

For $\sqrt{s} = 200\text{GeV}$

$$\begin{aligned} x(y) &= 0.5 \left[\frac{m}{200}(\exp y - \exp(-y)) + \sqrt{\left(\frac{m}{200}(\exp y - \exp(-y))\right)^2 + 4a} \right] \\ \frac{dx(y)}{dy} &= \frac{M}{400}(\exp y + \exp(-y)) \left[1. + \frac{\frac{M}{200}(\exp y + \exp(-y))}{\sqrt{\left(\frac{M}{200}(\exp y - \exp(-y))\right)^2 + 4a}} \right]. \end{aligned} \quad (12)$$

Using Eqs(10,11,12), with the parton distribution functions given in Eq(8), we find $d\sigma/dy$ for $Q=3$ GeV, $\lambda = 0$ and $\lambda = 1$ the results for J/Ψ shown in Figure 4.

Figure 4: $d\sigma/dy$ for $Q=3$ GeV, $E=200$ GeV unpolarized p-p collisions producing J/Ψ with $\lambda = 0, \lambda = 1$

Note that the shape of $d\sigma/dy$ is consistent with the BNL-RHIC-PHENIX detector rapidity distribution[7].

For $\Psi'(2S)$ the results are shown in Figure 5.

Figure 5: $d\sigma/dy$ for $Q=3$ GeV, $E=200$ GeV unpolarized p-p collisions producing $\Psi'(2S)$ with $\lambda = 1, \lambda = 0$

The results for $d\sigma/dy$ shown in Figure 4. labeled $\Psi'(2S)(a)$ are obtained by using for the standard nonperturbative matrix element=0.039 times the matrix elements for J/Ψ production; while the results labeled $\Psi'(2S)(b)$ is obtained by using the matrix element derived using the result that the $\Psi'(2S)$ is approximately 50% a hybrid with the enhancement is at least a factor of π , as discussed above.

3.2 Upsilon Production Via Unpolarized p-p Collisions at $E=\sqrt{s}=38.8$ GeV at Fermilab

Since the $\Upsilon(nS)$ states have not been resolved at BNL-RHIC at the present time, we consider $\Upsilon(nS)$ state production at 38.8, which has been measured at Fermilab[13, 14]

For $Q=10$ GeV, using the parton distributions given in Eq(9) and Eqs(10,11) for helicity $\lambda = 0, \lambda = 1$, with $A_\Upsilon = 5.66 \times 10^{-4}$ nb and $a = 6.64 \times 10^{-2}$, we obtain $d\sigma/dy$ for $\Upsilon(nS)$ production.

The results for $\Upsilon(1S)$, $\Upsilon(2S)$ are shown in Figure 6, and for $\Upsilon(3S)$ in Figure 7.

Figure 6: $d\sigma/dy$ for $Q=10$ GeV, $E=38.8$ GeV unpolarized p-p collisions producing $\Upsilon(1S)$, $\Upsilon(2S)$ with $\lambda=0$, $\lambda=1$

Figure 7: $d\sigma/dy$ for $Q=10$ GeV, $E=38.8$ GeV unpolarized p-p collisions producing $\Upsilon(3S)$ with $\lambda=0$, $\lambda=1$

In Figure 6 $d\sigma/dy$ for $\Upsilon(1S)$ and $\Upsilon(2S)$ are obtained using the standard model for the matrix elements. In figure 7 the results for $d\sigma/dy$ for the standard model are labelled $\Upsilon(3S)a$, while the results for the hybrid model are labelled $\Upsilon(3S)b$.

It should be noted that the ratios of $d\sigma/dy$ for $\Psi'(2S)$, shown in Figure 5 and $\Upsilon(3S)$, shown in Figure 7 for the hybrid theory vs. the standard are our most significant results, as there are uncertainties in the absolute magnitudes and shapes of $d\sigma/dy$ on the scenerios, as well as the magnitudes of the matrix elements. This is discussed in the following subsection.

3.3 Dependence of $d\sigma/dy$ on scenerios

As stated above, our calculations make use of scenerio 2 of Ref[15]. It is important for us to point out that our main objective in the present work is to derive the relative magnitudes of the $\Psi'(2S)$ and $\Upsilon(3S)$ cross sections in our mixed heavy hybrid theory, vs standard quark models for these states. To illustrate this, we show Fig. 4 from Nayak and Smith' 2006 publication[15]. Scenerios 1, 2, 3 are defined by $1 < O_8^\Phi(^3P_0) >= < O_8^\Phi(^1S_0) >= .0087GeV^3$, $2 < O_8^\Phi(^3P_0) >=0$ and $< O_8^\Phi(^1S_0) >=.039GeV^3$, and $3 < O_8^\Phi(^3P_0) >= .01123GeV^3$ and $< O_8^\Phi(^1S_0) >= 0$. See Ref[15] for the form of Eq(1) with the three scenerios.

Figure 8: $d\sigma/dy$ for $Q= 3$ GeV, $E=200$ GeV polarized p-p collisions with $\lambda = 1$ producing J/Ψ . Scenerios 1, 2, 3 are shown with solid, dashed, and dotted curves, from Ref[15]

As one can see from Figure 8, the shapes and magnitudes of $d\sigma/dy$ depends on the scenerios, but this is not a problem in the present work, since we are mainly interested in ratios of cross sections; and our main problem with the shape (see Figs. 9 and 10) are for polarized Ψ production as in Ref[15].

4 Polarized p-p collisions at 200 GeV at BNL-RHIC

For polarized p-p collisions the equations for $\frac{d\sigma_{pp \rightarrow \Phi(\lambda=0)}}{dy}$ and $\frac{d\sigma_{pp \rightarrow \Phi(\lambda=1)}}{dy}$ are the same as Eqs(10,11) with the parton distribution functions f_g and f_q given in Eqs(8,9) replaced by Δf_g and Δf_q , the parton distribution functions for longitudinally polarized p-p collisions.

A fit to the parton distribution functions for polarized p-p collisions for Q=3 GeV obtained from CTEQ6[17] in the x range needed for $\sqrt{s}=200$ GeV is

$$\begin{aligned}\Delta f_g(x) &\simeq 15.99 - 700.34x + 13885.4x^2 - 97888.x^3 \\ \Delta f_d(x) &\simeq -5.378. + 205.60x - 4032.77x^2 + 28371.x^3 \\ \Delta f_u(x) &\simeq 8.44 - 292.19x + 5675.16x^2 - 39722.x^3 \\ \Delta f_{\bar{u}}(x) &\simeq -1.447 + 64.67x - 1268.24x^2 + 8878.32x^3 \\ \Delta f_{\bar{d}}(x) &= \Delta f_{\bar{u}}(x),\end{aligned}\tag{13}$$

and for Q=10 GeV, which we do not use in the present work, as the $\Upsilon(nS)$ are not resolved at BNL-RHIC,

$$\begin{aligned}\Delta f_{g10}(x) &\simeq 28.98 - 1435.47x + 29533.5x^2 - 211440.x^3 \\ \Delta f_{d10}(x) &\simeq -6.074 + 241.57x - 4762.04x^2 + 33604.4x^3 \\ \Delta f_{u10}(x) &\simeq 9.88 - 348.632x + 6729.49x^2 - 47058.x^3 \\ \Delta f_{\bar{u}10}(x) &\simeq -1.552 + 75.731x - 1531.97x^2 + 10896.6x^3 \\ \Delta f_{\bar{d}10}(x) &= \Delta f_{\bar{u}10}(x).\end{aligned}\tag{14}$$

The differential rapidity distribution for polarized p-p collisions are

$$\frac{d\Delta\sigma_{pp \rightarrow \Phi(\lambda=0)}}{dy} = -A_\Phi \frac{1}{x(y)} \Delta f_g(x(y), 2m) \Delta f_g(a/x(y), 2m) \frac{dx}{dy},\tag{15}$$

$$\begin{aligned}\frac{d\Delta\sigma_{pp \rightarrow \Phi(\lambda=1)}}{dy} &= -A_\Phi \frac{1}{x} [\Delta f_g(x(y), 2m) \Delta f_g(a/x(y), 2m) - 0.613(\Delta f_d(x(y), 2m) \\ &\quad \Delta f_{\bar{d}}(a/x(y), 2m) + \Delta f_u(x(y), 2m) \Delta f_{\bar{u}}(a/x(y), 2m))] \frac{dx}{dy}.\end{aligned}\tag{16}$$

For polarized p-p collisions, Q=3 GeV, the results for $d\Delta\sigma/dy$ for J/Ψ production using the standard model are shown in Figure 9; while for $\Psi'(2S)$ the results are shown in Figure 10. As above, the curves labelled $\Psi'(2S)a$ and are the standard model results, while that labelled $\Psi'(2S)b$ are the results for a mixed hybrid. The enhancement from active glue is once more quite evident. Since $\Upsilon(nS)$ states have not been resolved at BNL-RHIC, where polarized p-p collisions were measured, we do not calculate $d\Delta\sigma/dy$ for $\Upsilon(nS)$ states.

Once again, we stress that it is the ratios of $d\Delta\sigma/dy$ that is most significant, as there is uncertainty both the absolute magnitudes and shapes. Note that $d\Delta\sigma/dy$ is expected to have a maximum at $y=0$. As in N-S for polarized J/Ψ production, $d\Delta\sigma/dy < 0$ but there is a minimum at $y=0$ in absolute value for our results with scenerio 2. (See preceeding subsection on dependence on scenerios.)

Figure 9: $d\Delta\sigma/dy$ for $Q=3$ GeV, $E=200$ GeV polarized p-p collisions producing J/Ψ , with $\lambda = 0, \lambda = 1$

Figure 10: $d\Delta\sigma/dy$ for $Q= 3$ GeV, $E=200$ GeV polarized p-p collisions producing $\Psi'(2S)$ with $\lambda = 0, \lambda = 1$

5 Upsilon Production Via Unpolarized p-p Collisions at 7.26 TeV at LHC-CMS and 38.8 GeV at Fermilab

The cross sections for $\Upsilon(nS)$ state production in p-p collisions have been measured at 2.26 TeV at the LHC-CMS[12] and at 38.8 GeV at Fermilab[13]. In this subsection we calculate the cross sections for $\Upsilon(nS)$ production, with $n=1, 2, 3$. Then we use our theory that $\Upsilon(3S)$ is a hybrid to estimate the ratios of cross section. Since we are using scenerio 2 with $\langle O_8^\Phi(^3P_0) \rangle = 0$, the $\lambda = 0$ helicity dominates the cross section[15], and we drop the $\lambda = 1$ terms. From Eq(5), for $\lambda = 0$, the cross section is determined from

$$\sigma_{pp \rightarrow \Phi(\lambda=0)} = A_\Phi \int_a^1 \frac{dx}{x} f g(x, 2m) f g(a/x, 2m) .$$

We use this to estimate the ratios of the $\Upsilon(2S)$ and $\Upsilon(3S)$ production cross sections to the $\Upsilon(1S)$ production cross section for 2.76 TeV and 38.8 GeV.

5.1 Upsilon Production Via Unpolarized p-p Collisions at 7.26 TeV

For $\sqrt{s}=2.76$ TeV, for $\Upsilon(nS)$ production,

$$\begin{aligned} a &= 1.31 \times 10^{-5} \\ A_\Upsilon &= 1.12 \times 10^{-7} . \end{aligned} \tag{17}$$

The cross sections for $\Upsilon(nS)$ state production in p-p collisions have been measured at 2.26 TeV at the LHC-CMS[12] and at 38.8 GeV at Fermilab[13]. In this subsection we calculate the cross sections for $\Upsilon(nS)$ production, with $n=1, 2, 3$. Then we use our theory that $\Upsilon(3S)$ is a hybrid to estimate the ratios of cross section. Since we are using scenerio 2 with $\langle O_8^\Phi(^3P_0) \rangle = 0$, the $\lambda = 0$ helicity dominates the cross section[15], and we drop the $\lambda = 1$ terms. From Eq(5), for $\lambda = 0$, the cross section is determined from

$$\sigma_{pp \rightarrow \Phi(\lambda=0)} = A_\Phi \int_a^1 \frac{dx}{x} f g(x, 2m) f g(a/x, 2m) .$$

From this we find

$$\sigma_{pp \rightarrow \Upsilon(1S)} \simeq 0.85 \text{ nb} \tag{18}$$

What is significant for the present work are the ratios of the (1S), (2S), (3S) state production. In the preceeding sections we used estimates from the wave functions to find these ratios for the differential cross section. In the present section we make use of experimental results from the Fermilab experiment[13] for the ratio of $\sigma(\Upsilon(2S))/\sigma(\Upsilon(1S))$, since the 2S and 1S states are given by the standard model, and $\sigma(\Upsilon(3S))/\sigma(\Upsilon(1S)) = N3 \times \sigma(\Upsilon(2S))/\sigma(\Upsilon(1S))$, as discussed in Section 2. Therefore, our estimate of the standard model is

$$\begin{aligned}
\sigma(\Upsilon(2S))/\sigma(\Upsilon(1S)) &\simeq 0.27 \text{ standard} \\
\sigma(\Upsilon(3S))/\sigma(\Upsilon(1S)) &\simeq 0.04 \text{ standard, giving} \\
\frac{\sigma(\Upsilon(2S)) + \sigma(\Upsilon(3S))}{\sigma(\Upsilon(1S))} &\simeq 0.31 \text{ standard}
\end{aligned} \tag{19}$$

On the other hand, in our mixed hybrid theory with the $\Upsilon(3S)$ about 50% hybrid[8], we would expect a factor of $\pi^2/4$ in the matrix element, and therefore a factor of about 2.45 for the $\Upsilon(3S)$ cross section compared to the standard model.

This results in our estimate

$$\frac{\sigma(\Upsilon(2S)) + \sigma(\Upsilon(3S))}{\sigma(\Upsilon(1S))} = 0.52, \tag{20}$$

Compared to the LHC-CMS result[12] that this ratio is $0.78_{-0.14}^{+0.16} \pm .02$. while in the standard model it would be about 0.31.

5.2 Upsilon Production Via Unpolarized p-p Collisions at 38.8 GeV

Our study of the 38.8 Upsilon production is similar to the preseeded one for the LHC-CMS 2.76 TeV experiments. Our result for the $\sigma(\Upsilon(3S))/\sigma(\Upsilon(1S))$ expected at 38.8 GeV in the standard model, see Eq(19), compared to our mixed hybrid theory:

$$\begin{aligned}
\frac{\sigma(\Upsilon(3S))}{\sigma(\Upsilon(1S))} &\simeq 0.04 \text{ standard} \\
\frac{\sigma(\Upsilon(3S))}{\sigma(\Upsilon(1S))} &\simeq 0.147 - 0.22 \text{ hybrid}
\end{aligned} \tag{21}$$

compared to the experimental result[13] of about 0.12 to 0.16

6 Conclusions

We have applied the mixed hybrid theory for heavy quark states and predict that the cross sections for production of the charmonium $\Psi'(2S)$ state in 200 GeV p-p collisions and bottomonium $\Upsilon(3S)$ states in 38.8 GeV p-p collisions are much larger than the standard model. We have also estimated ratio of cross sections for 2.76 TeV and 38.8 GeV experiments, and our prediction for the $\Upsilon(3S)$ production cross section is larger than the standard model, and closer to the experimental values.

Because of the importance of gluonic production in processes in a Quark Gluon Plasma, this could lead to a test of the creation of QGP in RHIC. In order to treat the production of heavy mixed hybrid states via the QGP, however, we

must redo the QCD calculation using finite temperature field theory, as the properties of both the standard and hybrid components of the $\Psi'(2S)$ and $\Upsilon(3S)$, as well as the properties of the J/Ψ and the other $\Upsilon(nS)$ states, are modified by the temperature during the QCD phase transition. This is a project for future research.

Acknowledgments

This work was supported in part by a grant from the Pittsburgh Foundation, and in part by the DOE contracts W-7405-ENG-36 and DE-FG02-97ER41014.

References

- [1] CDF Collaboration, arXiv:hep-ex/9412013; Phys. Rev. Lett. **79**, 578 (1997)
- [2] CDF Collaboration, T. Affolder et al, Phys. Rev. Lett. **85**, 2886 (2000)
- [3] P.L Cho and A.K. Leibovich, Phys. Rev. **D 53**, 150 (1996)
- [4] E. Braaten and Y-Q Chen, Phys. Rev. **D 54**, 3216 (1996)
- [5] E. Braaten and S. Fleming, Phys. Rev. Lett. **74**, 3327 (1995)
- [6] G.C. Nayak, M.X. Liu, and F. Cooper, Phys. Rev. **D 68**, 034003 (2003)
- [7] F. Cooper, M.X. Liu, and G.C. Nayak, Phys. Rev. Lett. **93**, 171801 (2004)
- [8] L.S. Kisslinger, Phys. Rev. **D 79**, 114026 (2009)
- [9] L.S. Kisslinger, D. Parno, and S. Riordan, Adv. High Energy Phys. 2009:98231 (2009)
- [10] CDF Collaboratin, arXiv:hep-ex/9412013; Phys. Rev. Lett. **79**, 578 (1997)
- [11] H. Vogel, Proceedings of 4th Flavor Physics and CP Violation Conference (FPCP'06) (2006)
- [12] The CMS Collaboration, arXiv:1105.4894 (2011)
- [13] G. Moreno *et al*, Phys. Rev. **D 43**, 2815 (1991)
- [14] P. L. McGaughey *et al*, Phys. Rev. **D 50**, 3038 (1994)
- [15] G.C. Nayak and J. Smith, Phys. Rev. **D 73**, 014007 (2006)
- [16] E. Merzbacher, "Quantum Mechanics", John Wiley and Sons (1970)
- [17] CTEQ6: hep.pa.msu.edu/cteq/public/cteq6.html

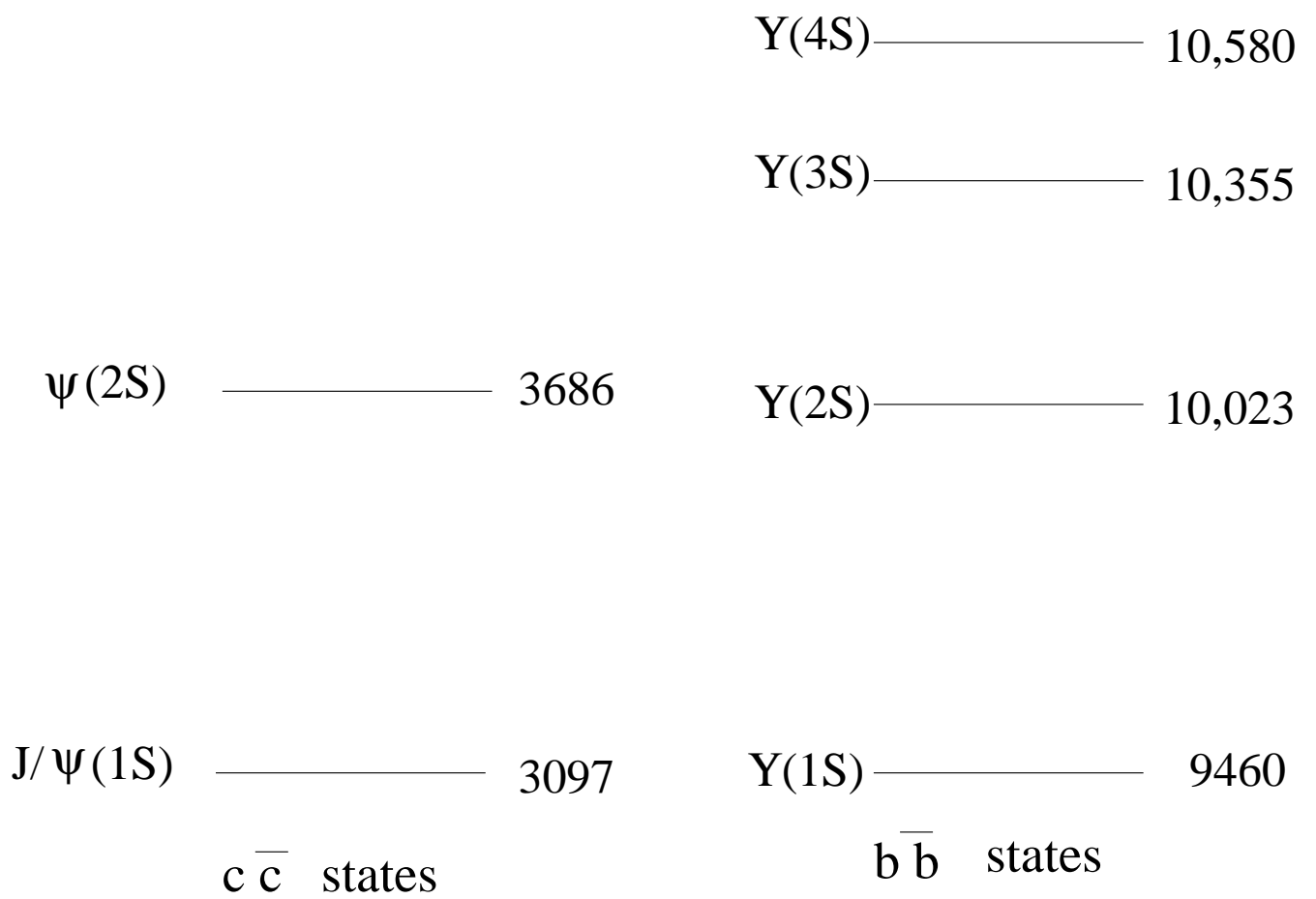
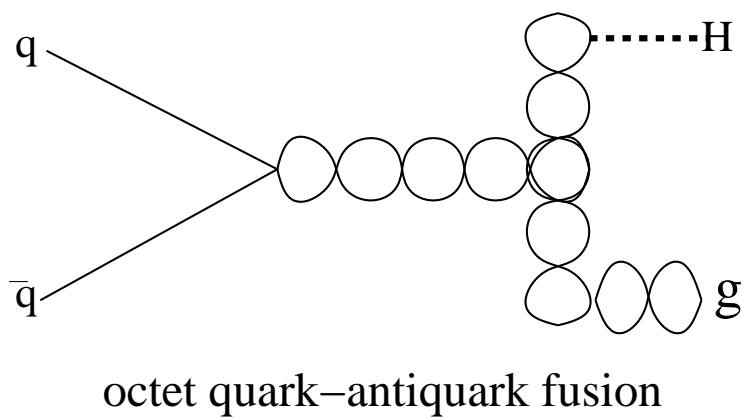
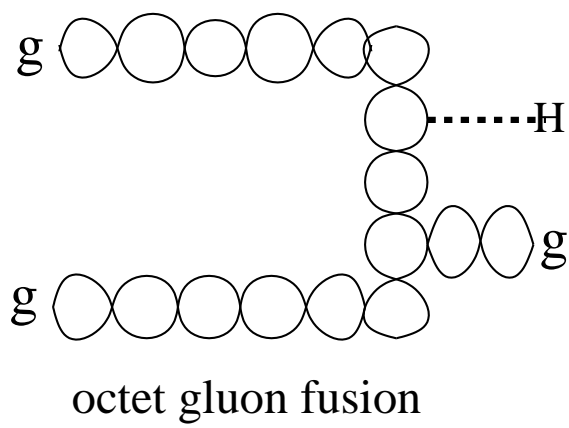
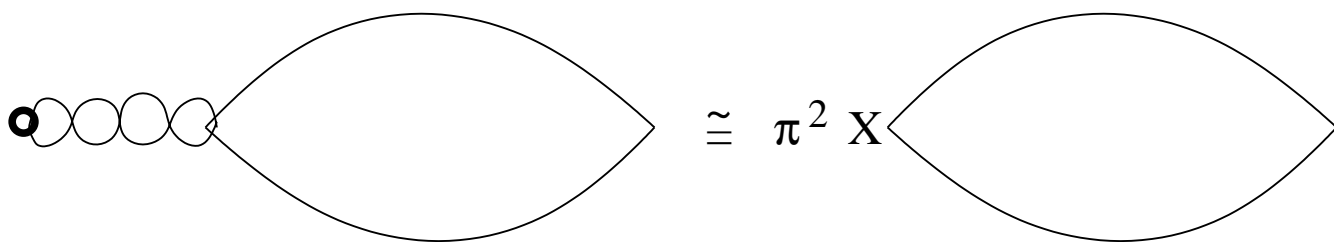


Figure 1 DH10962 24OCT11





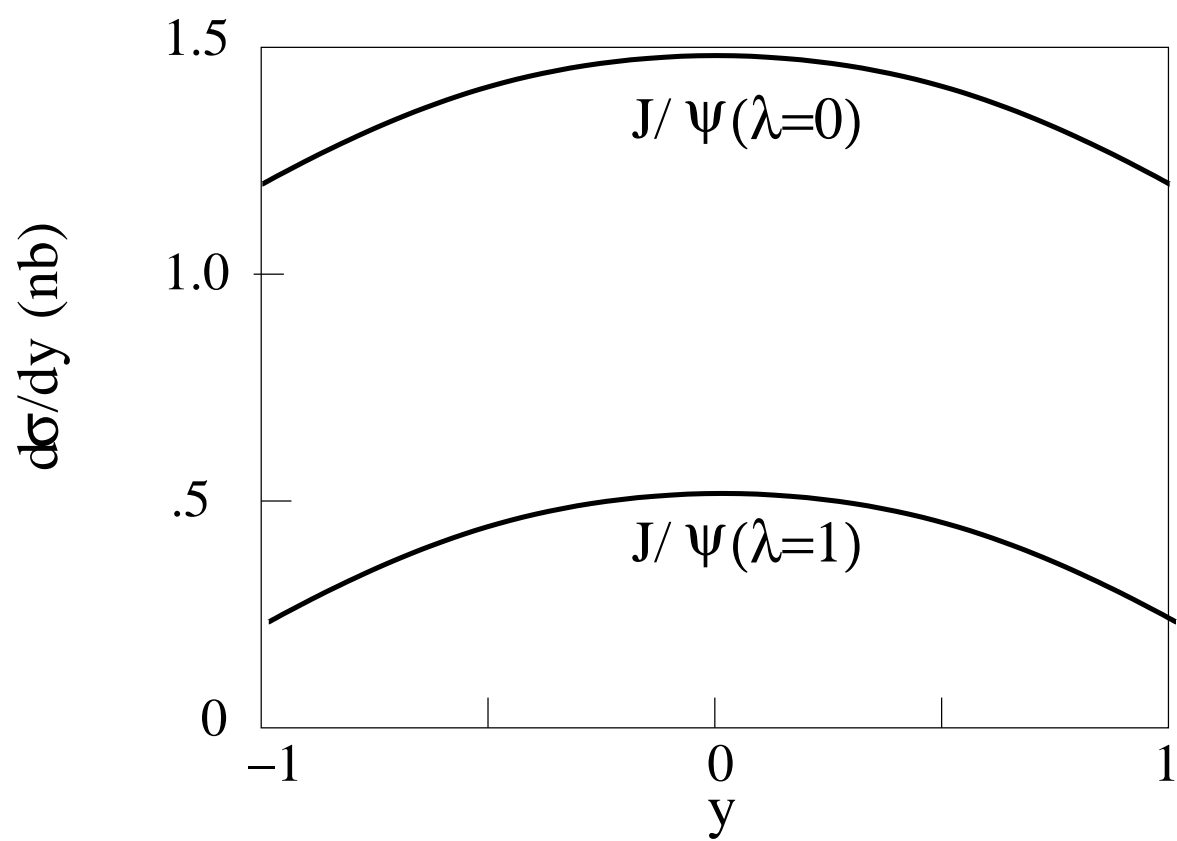


Figure 4 DH10962 24OCT11

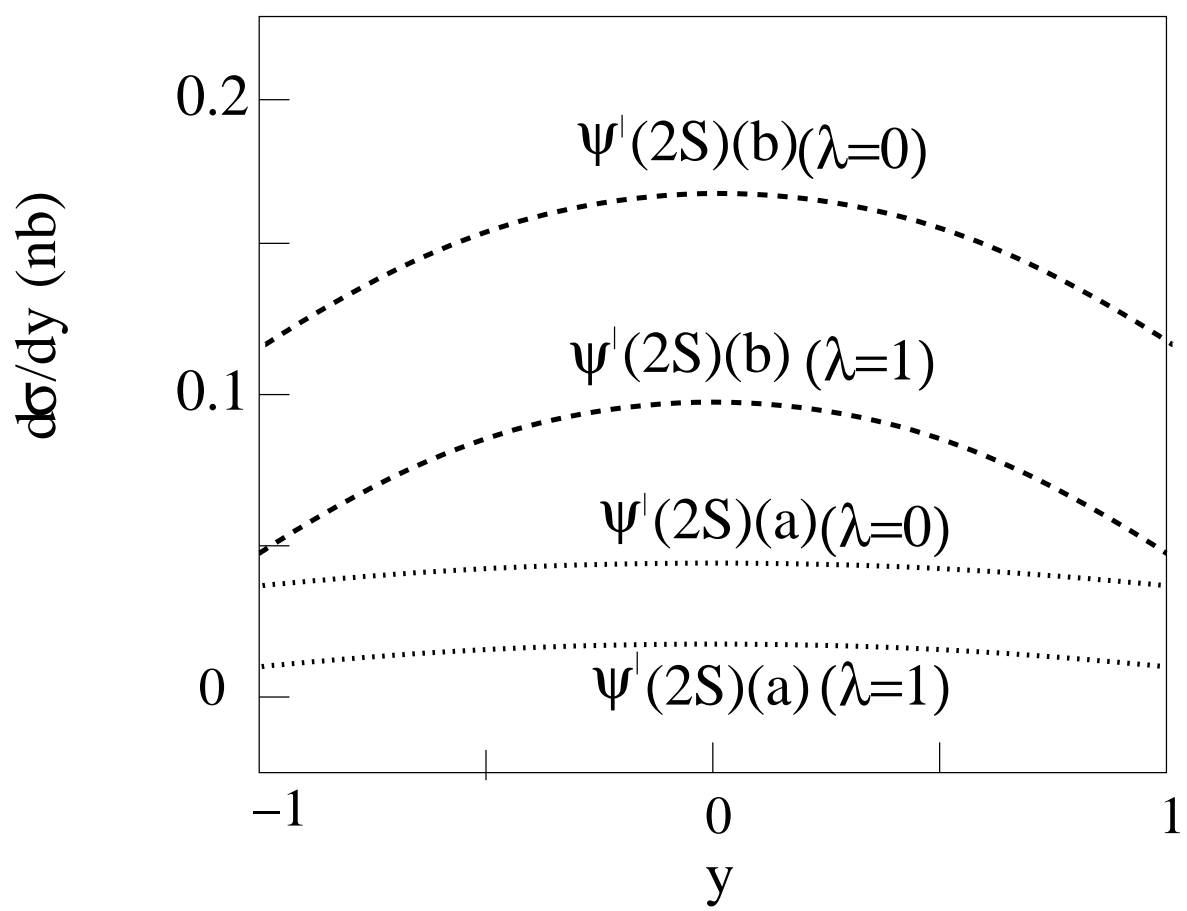


Figure 5 DH10962 24OCT11

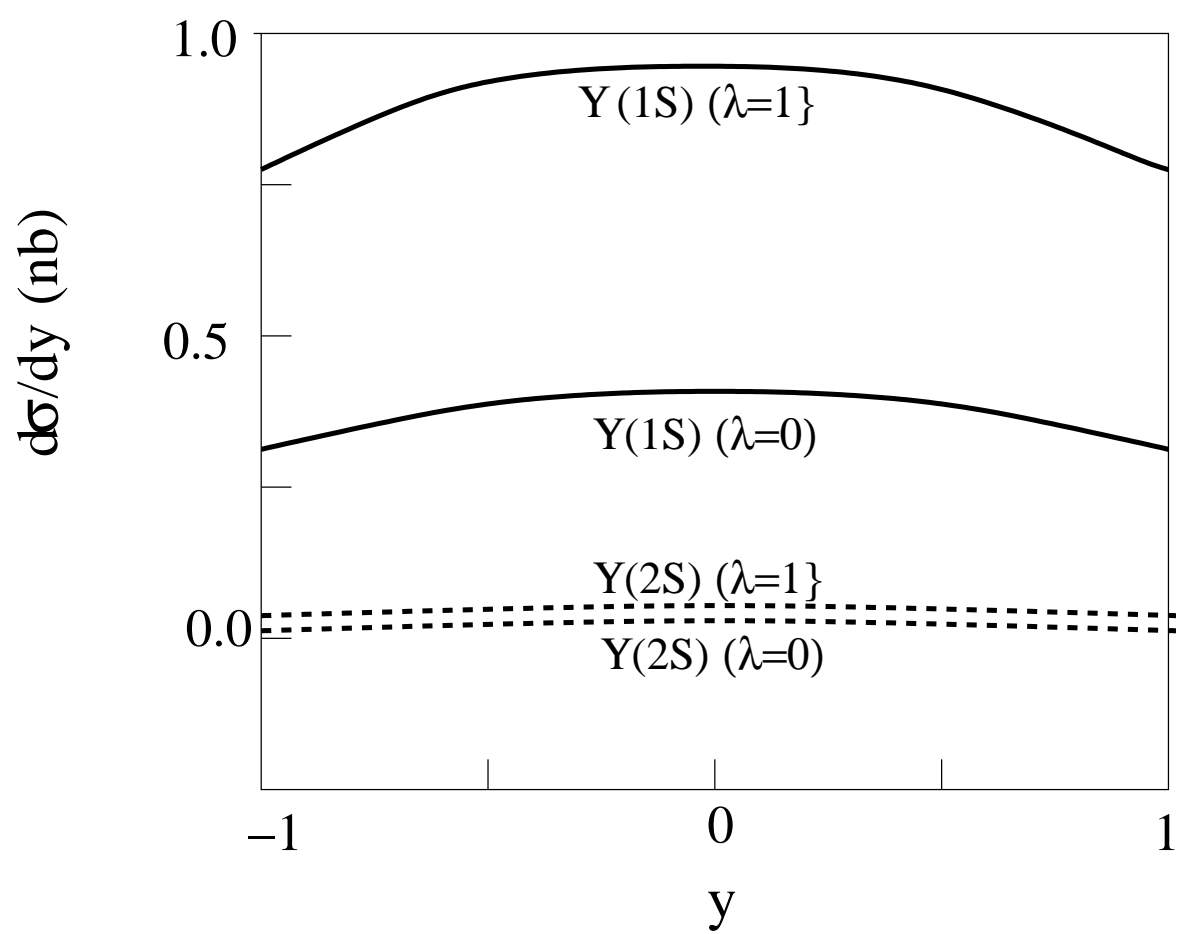


Figure 6 DH10962 24OCT11

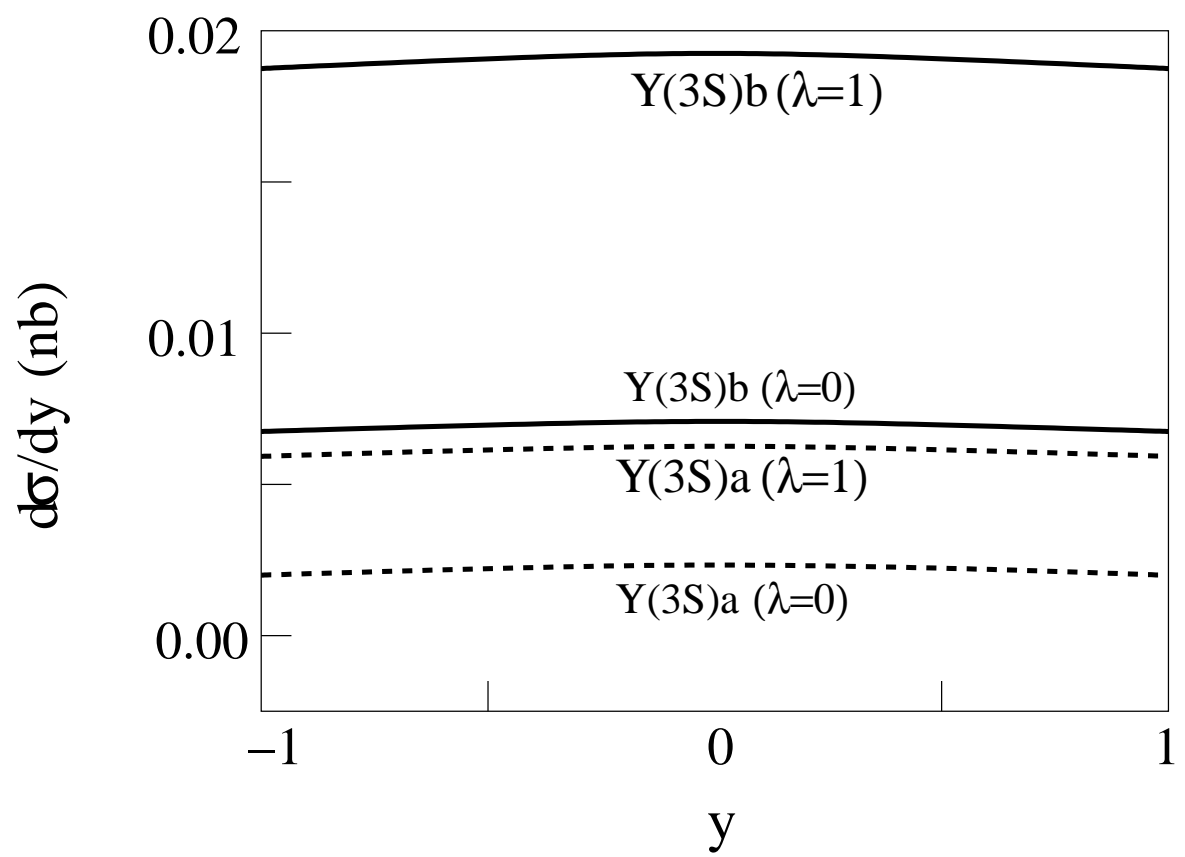


Figure 7 DH10962 24OCT11

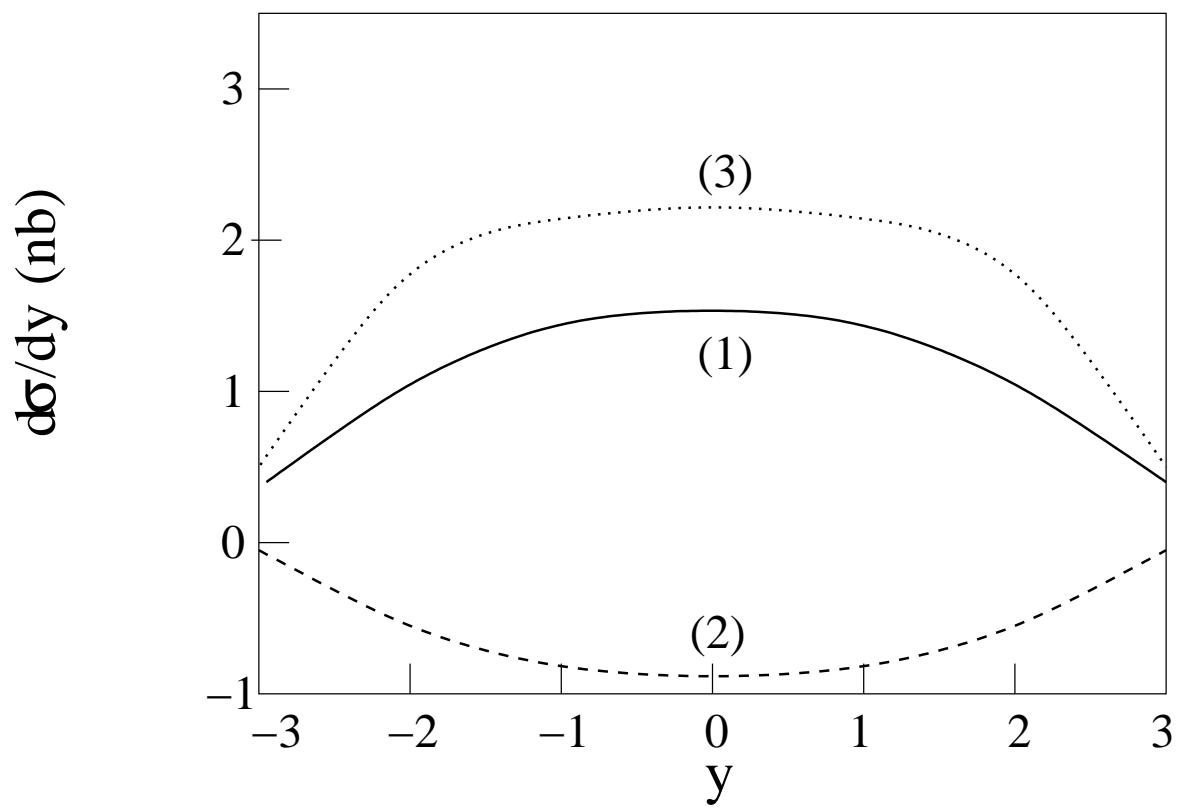


Figure 8 DH10962 24OCT11

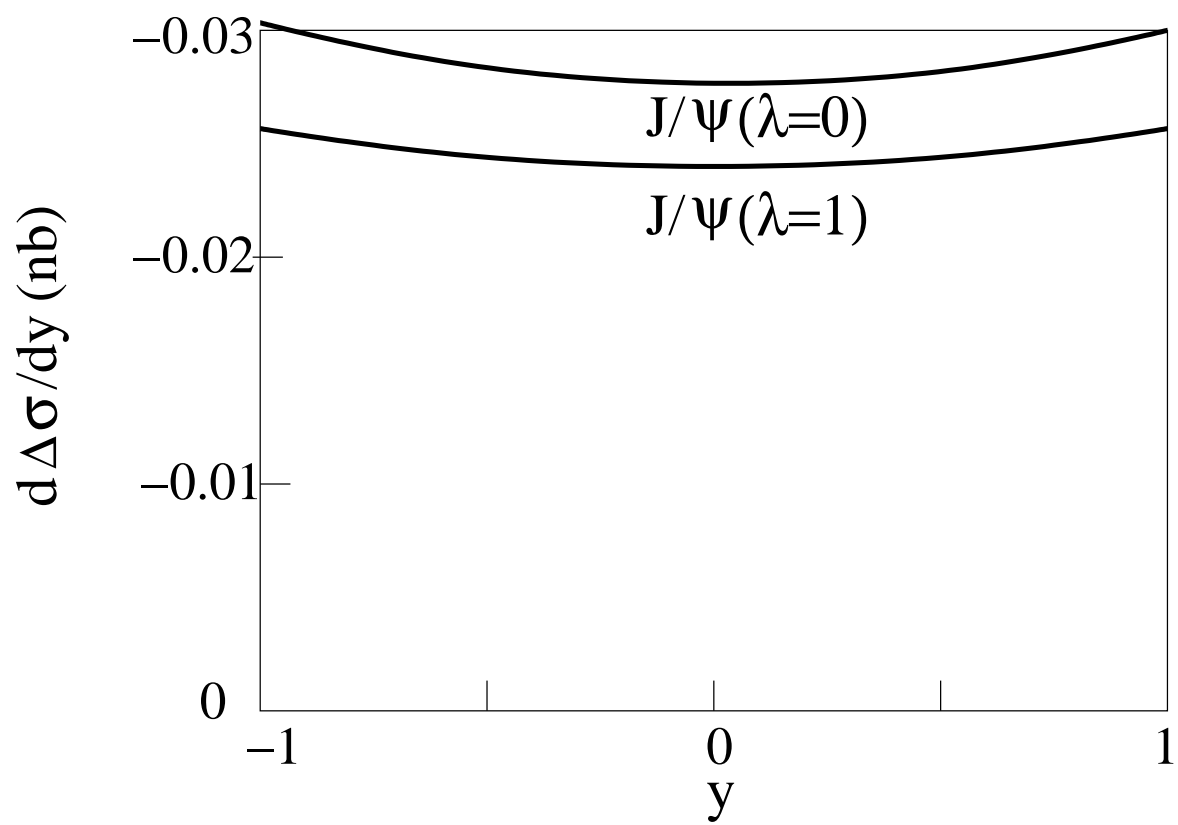


Figure 9

DH10962

24OCT11

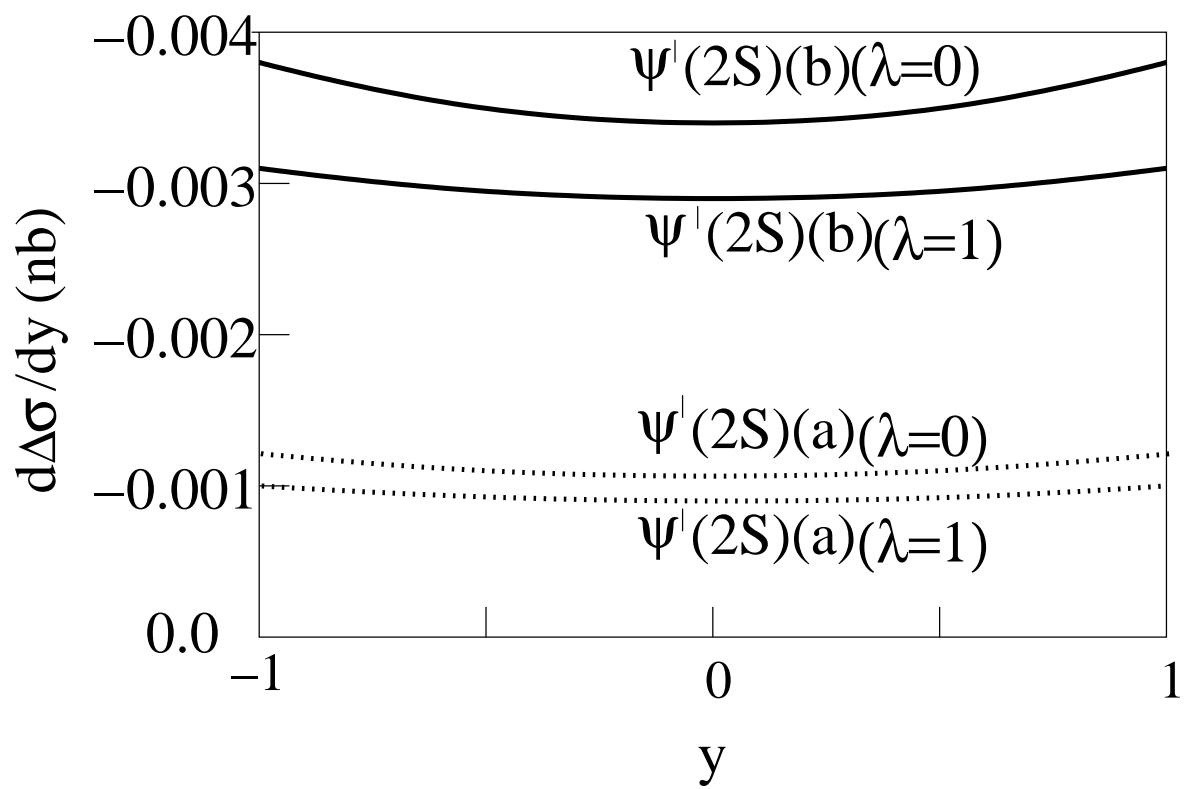


Figure 10 DH10962 24OCT11